CREATION AND PRESERVATION OF A SEA ICE CLIMATE DATA RECORD

YEAR 2 PROGRESS REPORT

1 MAY 2008 – 30 APRIL 2009

NOAA OAR-CPO-2007-2000636
SCIENTIFIC DATA STEWARDSHIP PROGRAM

SUBMITTED 3 JUNE 2009

PRINCIPAL INVESTIGATOR:
Walter N. Meier
walt@nsidc.org
303-492-6508

CO-INVESTIGATORS:
Florence Fetterer
fetterer@nsidc.org
303-492-4421

Julienne Stroeve
stroeve@kryos.colorado.edu
303-492-3584

Ruth Duerr
rduerr@nsidc.org
303-735-0136

National Snow and Ice Data Center
Cooperative Institute for Research in the Environmental Sciences
University of Colorado
UCB 449
Boulder, CO 80309
Fax: 303-492-2468

SUMMARY OF OVERALL PROJECT OBJECTIVES

The primary objective of this project is to lay the groundwork for the creation of a sea ice extent/area/concentration climate data record. The current standard sea ice fields are produced from passive microwave satellite brightness temperature fields. These provide complete daily coverage of the polar regions since late 1978. This nearly 30-year record is one of the longer satellite climate records and is a key indicator of climate change. The Arctic has experienced a precipitous decline in sea ice extent, particularly during summer, over the three decade record (e.g., Meier et al., 2007; Comiso and Nishio, 2008). Recent years have been particularly low, culminating in an extreme record minimum in September 2007, with extents 40% below normal and over 20% below the previous record low (Stroeve et al., 2008; Comiso et al., 2008).

However, for several reasons, the sea ice record is not yet at a sufficient level to be considered a true Climate Data Record (CDR). There is not a single authoritative and accepted sea ice product. The products lack grid cell-level or even granule-level error estimates or quality assessments (a granule refers to a coherent set of data, e.g., a daily field of a parameter). Intersensor calibration, while carefully conducted, could be improved. Finally, the metadata for the products is not comprehensive and does not meet the modern standards.

This project aims to address these deficiencies to allow the eventual production of a sea ice CDR. Specifically, the project objectives, as outlined in the original proposal are:

1. Intercalibrate the SMMR-SSM/I with the AMSR-E record to use the most recent, highest technology sensor as a basis for the record. This will also include implementing the NASA Team 2 algorithm over the SSM/I record, where the required high frequency channels (85.5 GHz) exist.
2. Develop data quality fields to accompany the data fields. This will be done through a variety of methods including temporal history and spatial correlation of the concentration fields, ancillary data (e.g., melt onset fields), and further comparisons with other basin-scale sea ice fields (such as AMSR-E concentrations from NSIDC processing).
3. Implement improved metadata and preservation standards. These standards will be FGDC/ISO 19115 compliant at both the file and data set level. The ability to distribute these products in data formats popular with specific user communities will be provided (e.g., NetCDF, GRIB2).

The end result will be higher quality sea ice concentration fields with associated data quality estimates and quality metadata information that will provide long-term preservation and reduce long-term maintenance costs. The production of these fields will provide a stable authoritative climate record into the NPOESS era and beyond.

BACKGROUND

Sea ice estimates are produced from two widely used algorithms, the NASA Team (Cavalieri and Gloersen, 1984) and the Bootstrap (Comiso et al., 1997), both developed at the NASA Goddard Space Flight Center. There are also several other, less widespread, algorithms in use. For the newer NASA Advanced Microwave Scanning Radiometer for EOS (AMSR-E), an enhanced NASA Team algorithm (Markus and Cavalieri, 2000), commonly referred to as NASA Team 2, is employed. Each sea ice algorithm uses combinations of passive microwave frequencies and polarizations to estimate sea ice concentration (percent ice cover within a grid cell), but the algorithms are formulated in different ways and use different combinations of channels. Evaluations of the algorithms have found that some algorithms perform better in some locations and some parts of the year, but that no single algorithm is optimal for all conditions (Comiso et al., 1997; Meier, 2005).

Another deficiency of the sea ice products in relation to CDR standards is that error estimates or quality assessments are lacking. There are only general error estimates based on a few local validation campaigns. Studies have shown that the quality of individual concentration estimates can vary dramatically, even over short distances and timescales (e.g., Meier, 2005).

Table 1. Characteristics of multichannel passive microwave sensors used in production of sea ice products and potential future sources. F8, F11, F13 denote DMSP satellites on which SSM/I was included. All frequencies include channels for both horizontal and vertical polarization, except 21.0/22.2, which has only a vertically polarized channel. MIS is currently planned for NPOESS. †Much of F8 85.5 GHz data missing or of low quality. ‡F15 was used operationally until an issue with the 22.2 GHz frequency corrupted the sea ice algorithm. F17 will begin operational use for sea ice in June 2009..

Sensor	Years of Operation	T_b Frequencies (GHz)	Min. Gridded Conc. Cell Size (km)
SMMR	10/25/78-8/20/87	6.6, 10.7, 18.0, 21.0, 37.0	25
SSM/I F8	7/9/87-12/31/91	19.3, 22.2, 37.0, 85.5†	25
SSM/I F11	12/3/91-9/30/95	19.3, 22.2, 37.0, 85.5	25
SSM/I F13	5/3/95-present	19.3, 22.2, 37.0, 85.5	25
SSM/I F15‡	12/18/99-present	19.3, 22.2, 37.0, 85.5	25
SSMIS F17	3/28/2008-present	19.3, 22.2, 37.0, 89.0	25
AMSR-E	6/18/02-present	6.9, 10.7, 18.7, 23.5, 36.5, 89.0	12.5
MIS	Planned ~2015	6.0-183.0	12.5 or less

The current widely-used sea ice timeseries employ the Nimbus-7 Scanning Multichannel Microwave Radiometer (SMMR) from 1978 to 1987 and a series of Special Sensor Microwave/Imagers (SSM/I) on the Defense Meteorological Satellite Program (DMSP) F- series satellites beginning with F8 in 1987 (Table 1). Thus, creation of the long-term sea ice timeseries has required intersensor calibration across numerous sensors. This has been carefully done to assure good consistency over the records (Cavalieri et al., 1999). However, there are some limitations in the intercalibrations. First, some overlap periods were extremely short, as little as three weeks (F8 to F11). Most of the overlap periods (all except F8 to F11) have been in the boreal summer (austral winter). Thus any seasonality effects on the intercalibration could not be accounted for. Ideally, a one-year

overlap period should be used to cover the full range of annual variability. The sea ice products were not intercalibrated at the level of the sensor measurements (i.e., brightness temperature). Such an approach was unable to yield consistent results, so the intercalibration was done at the final product level to produce consistent sea ice extents. However, though extents were matched, inconsistency has been found in ice area fields.

Finally, the sea ice products lack comprehensive metadata, particularly at the grid cell or granule level. Current metadata includes basic product-level documentation and, for only some products, rudimentary granule-level information consisting of basic parameter information (date, parameter name, units, scaling, flag values).

YEAR TWO ACCOMPLISHMENTS

The Year Two accomplishments encompassed two major issues: (1) Development of data quality fields, and (2) Continued intersensor calibration development.

Task 1 – Development of data quality fields

1. Implemented eight sea ice concentration algorithms and used spread of estimates to develop basic uncertainty parameters for sea ice concentration and extent.
2. Implemented melt onset algorithm for a data quality flag to indicate degradation of sea ice concentration during the summer.
3. Presented results as invited speaker at American Geophysical Union 2008 Fall Meeting in San Francisco.
4. Co-chaired (with Sheldon Drobot and David Robinson) workshop on climate data records at AGU Fall Meeting to obtain feedback from users and start to develop key principles for sea ice CDR.
5. Submitted abstract to SPIE meeting.

Task 2 – Intersensor calibration

1. Acquired one year of overlap data from DMSP F13 SSM/I and DMSP F17 SSM/IS for intersensor calibration
2. Performed intersensor calibration between F13 and F17.
3. Compared sea ice extents from the NASA Team algorithm for F13 and F17.
4. Developed new method to optimally adjust algorithm tiepoints for highest consistency between sensor outputs.
5. Investigated effect of using brief time periods (a few weeks to a few months) for intercalibration as employed for previous sensor transitions compared to using a full-year available for F13-F17.
6. Prepared manuscript for submission on F13-F17 intersensor calibration and tiepoint adjustment. Paper will be submitted soon.

Other Ongoing Tasks

1. Continued discussion of collaboration on CDR development with Sheldon Drobot, University of Colorado, and David Robinson, Rutgers University.
2. Continued discussion with ESA EUMETSAT Satellite Application Facility for possible collaboration when their reanalysis is complete (planned for later in 2009).
3. Investigation of metadata standards.

Details on each task are discussed below:

Task 1 – Development of data quality fields

The initial approach for starting to develop data quality fields has been to implement several algorithms for sea ice concentration. The range in concentration values provides a rudimentary estimate of uncertainty in the overall passive microwave concentrations. At the ice edge, the number of algorithms that obtain ice (>15% threshold) versus those algorithms that do not obtain ice (<15% threshold) is an indication of the uncertainty in the ice edge location.

In all eight algorithms were implemented and run for 2007 and 2008:

1. NASA Team on SSM/I
2. NASA Team 2 from the AMSR-E standard product
3. AMSR-E Bootstrap algorithm
4. ASI 6.25 km 89 GHz frequency algorithm from University of Bremen
5. SSM/I Bootstrap
6. Bristol
7. Norsex
8. Cal/Val (AES-York)

The averages and standard deviations were calculated. The spread (standard deviation) gives some indication in the uncertainty in the products, both in total extent/area (Figures 1 and 2) over the whole basin as well as at a given pixel. In addition, a melt algorithm (Drobot and Anderson, 2001) was implemented to flag summer melt pixels. Of course, not all algorithms are equal and simply taking the average and standard deviation is a fairly naïve approach. However, this provides a good starting point. As work progress, worse performing algorithms can be discarded. Also, instead of a simple average, the algorithm outputs could be weighted to provide a more optimum output.

Spatial maps of the range of values from the algorithms (maximum-minimum concentration) provide an indication of where algorithms are consistent (less uncertainty) versus less consistent (higher uncertainty). Because melt significant affects the passive microwave signal, the melt flag also provides an indication of where the algorithms may be performing more poorly.

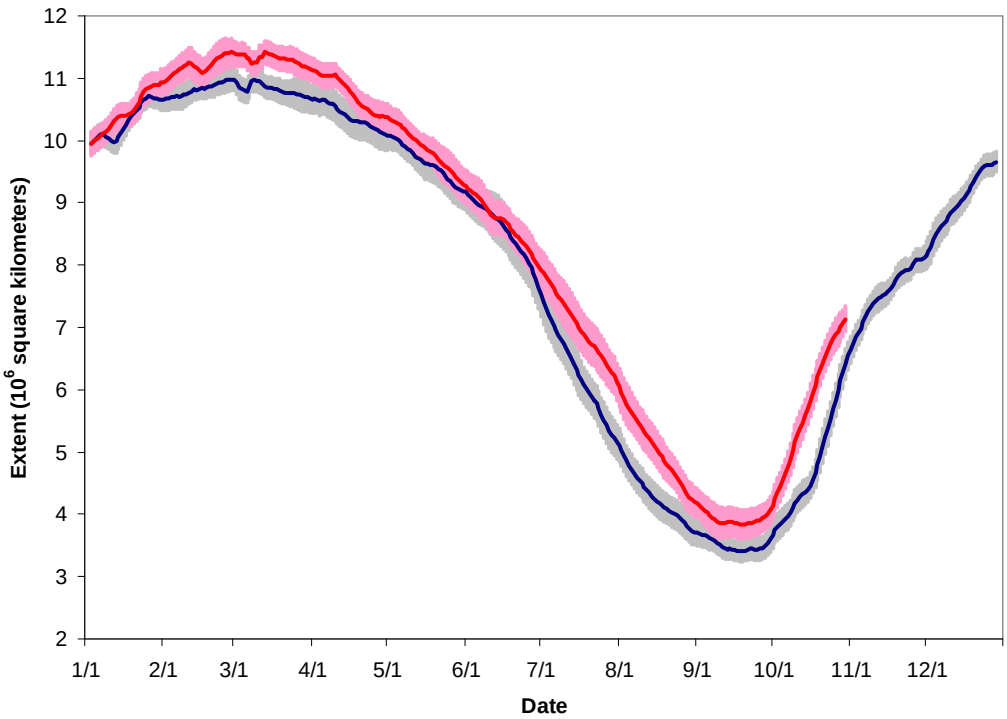

Figure 1. Sea ice average total extent and standard deviation for 2007 (blue line, gray envelope) and 2008 through 31 October (red line, pink envelope).

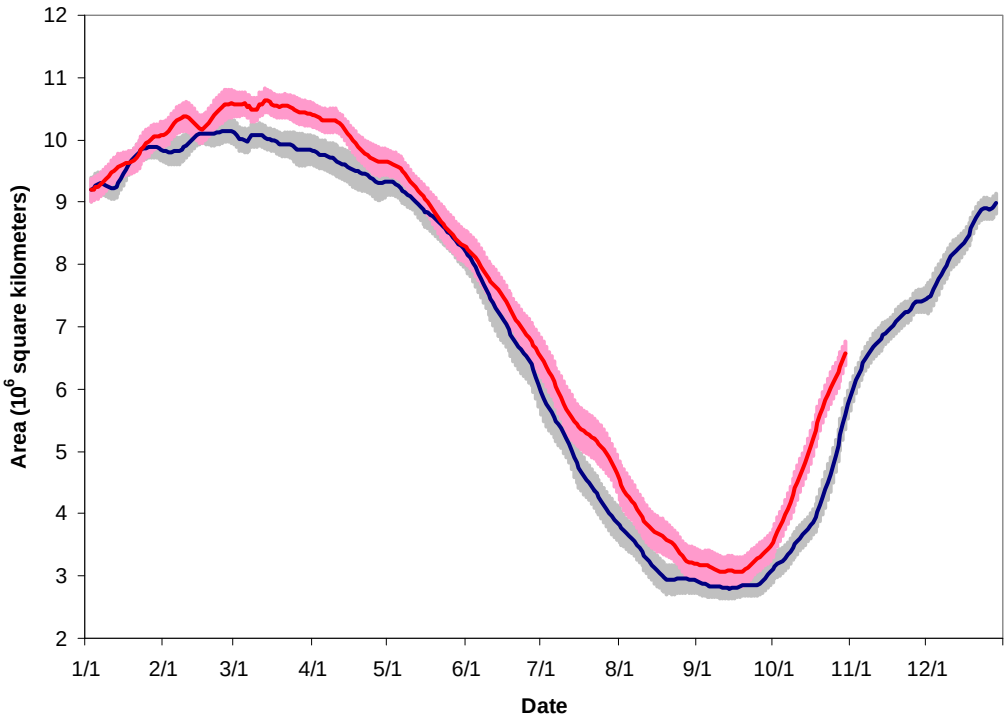

Figure 2. Sea ice average total area and standard deviation for 2007 (blue line, gray envelope) and 2008 through 31 October (red line, pink envelope).

The spatial maps indicate that in March, before melt has begun, the results of the algorithms are more consistent (Figure 3) over much of the Arctic. Once melt has begun, there is a much larger spread in the concentrations over most of the ice cover.

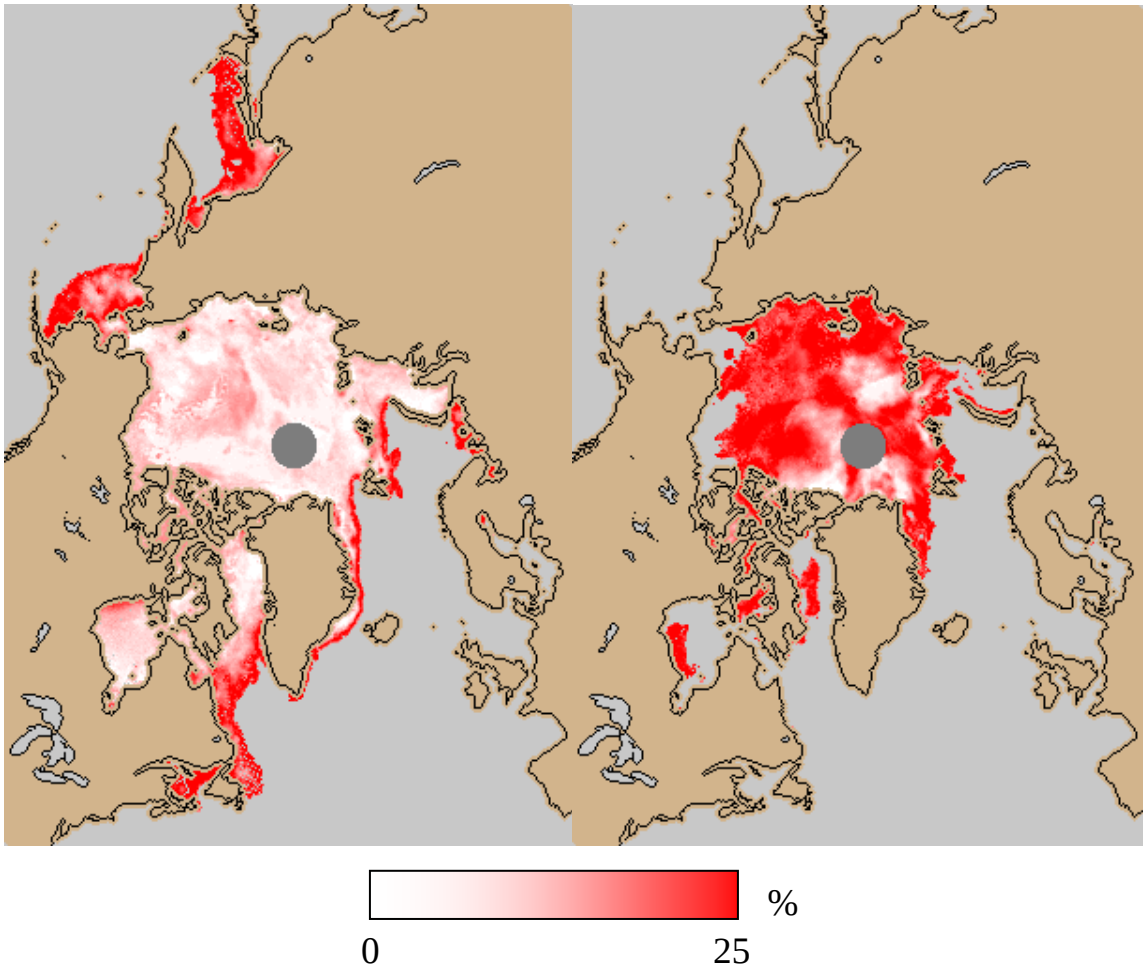

Figure 3. Sea ice concentration range for March 15 (left) and July 15 (right) 2008.

The melt onset flag provides a second quality check. When melt begins, the liquid water on the surface degrades the algorithm performance (some algorithms more than others). In addition another check was implemented where the total number of algorithms that show ice greater than 15% are counted. The more algorithms showing ice, the more confidence there is that there is truly ice in a given pixel. In Figure 4, a threshold of 4 out of the 8 algorithms needed to show ice for the field to consider a pixel was “possible ice”.

These results were presented at the American Geophysical Union 2008 Fall Meeting as an invited talk in a “Cryospheric Climate Data Records” session. At the meeting, there was also a side workshop co-hosted by the PI (along with S. Drobot, NCAR, and D. Robinson, Univ. Rutgers) to discuss cryospheric CDRs with the science community.

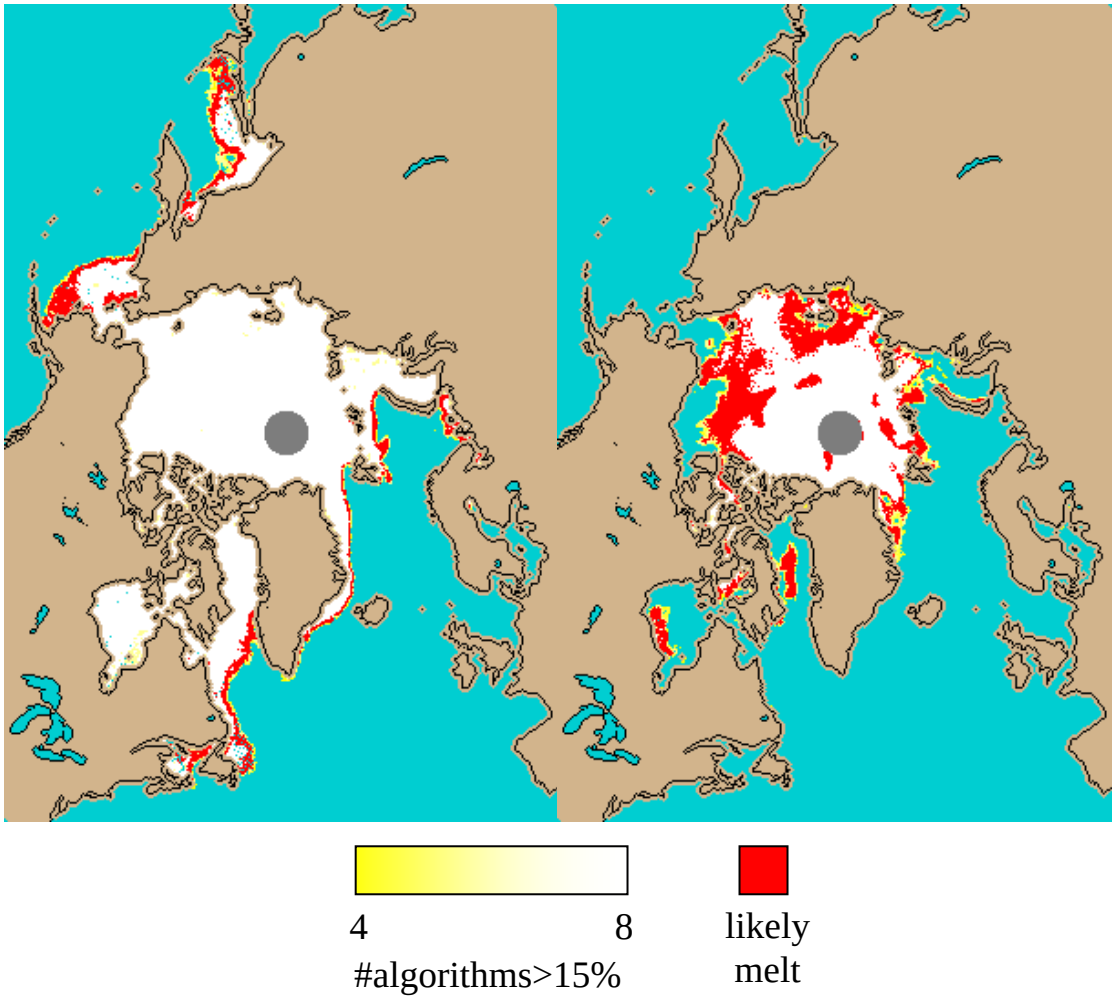

Figure 4. Quality field for sea ice for March 15 (left) and July 15 (right) 2008. The yellow band along the ice edge indicates where only some of the algorithms have ice. The red indicates that there is likely melt.

Task 2 – Intersensor calibration between F-13 and F-17

The SSM/I sensor on DMSP F-13 is well past its planned lifetime and is heading toward obsolescence. Sensor performance has been less than optimal since January 2008, though still reasonable to provide quality, mostly-complete sea ice fields. Thus, it was necessary to prepare to transition to the SSMIS sensor on DMSP F-17. F-17 data from the NOAA CLASS system (a new source for NSIDC) were obtained and intersensor calibration was performed. The methodology used for the calibration of the sea ice fields was similar to previous efforts. (Cavalieri, et al., 1999). However, some of the approaches were modified to provide a more objective and better documented intercalibration. The intercalibration was also done for a full year of overlap (1 April 2008 – 31 March 2009), the longest passive microwave overlap used for calibration. This long overlap encompasses a full seasonal cycle for both the Arctic and Antarctic. It also allows us to investigate the potential limitations resulting from using the shorter intercalibrations in the past. The results have been documented in a manuscript currently

in the final stages of preparation. It is expected to be submitted to IEEE Transactions on Geoscience and Remote Sensing or a similar journal in the next few weeks. The draft version of that manuscript is included in an appendix at the end of the report.

In mid-May 2009, the F-13 sensor performance started to degrade even further, to the point that it was unusable. At that point, F-17 was put into production with minimal disruption to the operational data stream. Some details on the transition can be found at: http://nsidc.org/arcticseaicenews/2009/060209.html.

PLANS FOR YEAR THREE OF THE PROJECT

There are several planned accomplishments for Year 3, including:

1. Continue intersensor calibration studies, particularly looking at possible improvements to previous intercalibrations during the SMMR-SSM/I era.
2. Implement NASA Team 2 algorithm and compare extents between F13, F17, and AMSR-E. Also, compare NASA Team 2 fields with NASA Team fields.
3. Continue developing grid cells- and granule-level error estimates and quality assessments. Instead of simply combining the eight algorithm outputs, more optimal schemes will be investigated.
4. Continue development of metadata standards.
5. Present results at the SPIE Optics and Photonics conference in San Diego, 2-6 August.
6. Submit peer-reviewed journal article describing the intersensor calibration and a second manuscript on other aspects of the CDR project.
7. Continue collaborations with S. Drobot and D. Robinson on their CDR project. Also continue collaborations with the EUMETSAT sea ice reanalysis project; their reanalysis is expected to be complete later this year and we will coordinate with them on possible mutually-beneficial collaborations.

REFERENCES

Cavalieri, D.J., and P. Gloersen, 1984. Determination of sea ice parameters with the Nimbus-7 SMMR, *J. Geophys. Res.*, 89(D4), 5355-5369.

Cavalieri, D.J., C.L. Parkinson, P. Gloersen, J.C. Comiso, and H.J. Zwally, 1999. Deriving long-term time series of sea ice cover from satellite passive-microwave multisensor data sets, *J. Geophys. Res.*,104(C7), 15,803-15,814.

Comiso, J.C., D.J. Cavalieri, C.L. Parkinson, and P. Gloersen, 1997. Passive microwave algorithms for sea ice concentration: A comparison of two techniques, *Rem. Sens. Env.*, 60, 357-384.

Comiso, J.C., and F. Nishio, 2008. Trends in the sea ice cover using enhanced and compatible AMSR-E, SSM/I, and SMMR data, *J. Geophys. Res.*, 113, C02S07, doi:10.1029/2007JC004257.

Comiso, J.C., C.L. Parkinson, R. Gersten, and L. Stock, 2008. Accelerated decline in the Arctic sea ice cover, *Geophys. Res. Lett.*, 35, L01703, doi:10.1029/2007GL031972.

Drobot, S., and M. Anderson, 2001. Comparison of interannual snowmelt onset dates with atmospheric conditions, *Ann. Glaciol.*, 33, 79-84.

Markus, T., and D.J. Cavalieri, 2000. An enhanced NASA Team sea ice algorithm, *IEEE Trans. Geosci. and Rem. Sens.*, 38(3), 1387-1398.

Meier, W.N., 2005. Comparison of passive microwave ice concentration algorithm retrievals with AVHRR imagery in Arctic peripheral seas, *IEEE Trans. Geosci. Rem. Sens.*, 43(6), 1324-1337.

Meier, W.N., J. Stroeve, F. Fetterer, 2007. Whither Arctic sea ice? A clear signal of decline regionally, seasonally, and extending beyond the satellite record, *Ann. Glaciol.*, 46, 428-434.

Stroeve, J., M. Serreze, S. Drobot, S. Gearheard, M. Holland, J. Maslanik, W. Meier, T. Scambos, 2008. Arctic sea ice extent plummets in 2007, *Eos, Trans. Amer. Geophys. Union*, 89(2), 13-14.

APPENDIX:

Manuscript on Intersensor Calibration

INTERSENSOR CALIBRATION BETWEEN F-13 SSM/I AND F-17 SSMIS SEA ICE ESTIMATES

Walter N. Meier, Siri Jodha Singh Khalsa, National Snow and Ice Data Center

Introduction

Since 1987 the Special Sensor Microwave/Imager (SSM/I) on the Defense Meteorological Satellite Platform (DMSP) has been a stalwart for tracking sea ice extent and area. Combined with the earlier Nimbus-7 Scanning Multichannel Microwave Radiometer (SMMR) record (1978-1987), satellite passive microwave has yielded an ongoing 30+ year timeseries of sea ice conditions. This is one of the longest satellite climate records available and has been a key indicator of climate change.

The timeseries is not created from a single sensor but rather is stitched together from SMMR and a series of SSM/I sensors on the DMSP F-series satellites. To provide a consistent, high-quality timeseries through the period of record, it is essential to perform an intercalibration between the sea ice products. This is accomplished by adjustments to algorithm coefficients. Historically, the period of overlap for the sensors has been short, limiting the intercalibration to a period of at most a few weeks. Thus, potential impacts from seasonal variability could not be accounted for. Ideally, at least an entire year of overlap should be used to fully account for intra-annual variations in sensor characteristics.

NSIDC Passive Microwave Products

Brightness Temperature Data

The National Snow and Ice Data Center currently archives a complete timeseries of SMMR and SSM/I brightness temperatures. Daily gridded brightness temperature fields on a 25-kilometer polar stereographic projection (tangent at 70° latitude) are produced via a “drop-in-the-bucket” composite using all swaths from the day from a given instrument and direction (ascending or descending orbit). NSIDC also produces brightness temperatures fields on EASE-Grid.

The archive consists primarily of data from a single satellite except for periods of overlap (Table 1). Early overlap periods were often very short. In more recent years, data from multiple SSM/I sensors are available, but have not been archived at NSIDC.

Satellite	Sensor	Dates of NSIDC Data	Overlap Days with Previous Sensor
Nimbus-7	SMMR	25 Oct 1978 – 20 Aug 1987	
DMSP F-8	SSM/I	9 Jul 1987 – 18 Dec 1991	22
DMSP F-11	SSM/I	3 Dec 1991 – 30 Sep 1995	16
DMSP F-13	SSM/I	30 May 1995 – present	123
DMSP F-17	SSMIS	28 Mar 2008 – present	365+

Table 1. NSIDC passive microwave brightness temperature archive, including the planned addition of F-17 SSMIS data. Note that SMMR provided data only every other day.

Polar Stereographic Sea Ice Products

NSIDC produces a standard near-real-team polar stereographic sea ice concentration product based on daily composite brightness temperatures. The product uses the NASA Team Algorithm (*Cavalieri et al.*, 1984; 1999). The algorithm uses ratios of channels to estimate the concentration of sea ice within a grid cell. It relies on empirically-derived coefficients, or 'tiepoints', for three pure surface types – an open water type and two sea ice types. In the Northern Hemisphere, the two sea ice types correspond to first-year ice (FYI) and multiyear ice (MYI). Due to little MYI coverage and differing ice conditions, in the Southern Hemisphere the sea ice types are simply denoted "Type A" and "Type B". NSIDC also archives sea ice products using the Bootstrap Algorithm (*Comiso et al.*, 1997).

Handling Passive Microwave Sensor Transitions

No single satellite sensor can provide a long-term climate record because sensor design lifetimes are limited to a few years. Though some sensors may last well beyond their planned missions, it will always be necessary to stitch together data from several sensors when compiling a long-term satellite climate record.

Due to differences in sensor design and satellite orbits, it is necessary to adjust sensor outputs to intercalibrate sensors and create a consistent record. For example, sensors on satellites in sun-synchronous orbits (including the Nimbus-7 and the DMSP F-series) with different ascending node crossing times will yield different results due to diurnal effects. Even if crossing times were the same and the sensors were the same there would still be differences simply due to uncontrollable variations during sensor construction.

Intersensor calibrations have been done on SSM/I brightness temperatures, these have generally focused on ocean products (e.g., *Wentz*, 1997). It has been found that these intercalibrations do not produce a sufficiently consistent sea ice product. A regression between brightness temperatures from the overlapping sensors is necessary to adjust the tiepoints for the new sensor (*Cavalieri et al.*, 1999). However, because grid cells are rarely a single surface type and because there can be substantial variation of the surface emissive properties (and hence the brightness temperature signal) even within a certain surface type, *Cavalieri et al.* (1999) found than an additional adjustment to some tiepoints was necessary.

NSIDC Near-Real-Time F-13 SSM/I to F-17 SSMIS Transition

Since January 2008, brightness temperatures from F-13 have been degraded by data gaps resulting from failing data recorders on the satellite. These data gaps appear most frequently in more southerly data where there are only one or two passes per day over the region. Thus, the effects are most pronounced near the winter maximums when the sea ice extends far southward. The resulting gaps in the sea ice fields can be filled in via a temporal interpolation from surrounding days.

However, because F-13 is well beyond its planned mission lifetime, NSIDC is switching to the F-17 Special Sensor Microwave Imager/Sounder (SSMIS) as its near-

real-time source for passive microwave sea ice products. The SSMIS is a new instrument replacing SSM/I on DMSP satellites. The lower frequency channels used in the sea ice products are the same as SSM/I, but there are additional higher frequency atmospheric sounding channels. The most substantial differences between the two sensors relevant for sea ice products are the swath width and the ascending node crossing time (Table 2).

	F-13 SSM/I	**F-17 SSMIS**
Channels for Sea Ice (GHz)	19.3, 22.0, 37.0	19.3, 22.0, 37.0
Altitude (km)	850	850
Asc. Node Local Crossing Time (as of 1 March 2009)	18:25	17:28
Swath Width (km)	1400	1700

Table 2. Relevant satellite and sensor characteristics for F-13 and F-17.

F-13 SSM/I and F-17 SSMIS Intercalibration

Since beginning distribution of near-real-time sea ice products, NSIDC has used F-13 SSM/I as the source data. With F-13 now well past the past the planned mission lifetime and likely to soon fail or be decommissioned, a near-real-time intersensor calibration for F-17 is necessary. This is the first time such a near-real-time calibration has been done for sea ice products.

The procedure NSIDC implemented essentially follows the method outlined by *Cavalieri et al.* (1999). A notable difference with the previous efforts however is that NSIDC conducted the intercalibration with a full year of overlap data (1 April 2008 – 31 March 2009). Thus, the intercalibration fully accounts for seasonal effects in the brightness temperature differences between the sensors.

The first step in the intercalibration is a regression between the brightness temperatures. This was done independently for all points in the Northern Hemisphere and Southern Hemisphere for each day on each channel used in the NASA Team algorithm (19V, 19H, 37V). The regression is a simply a linear best-fit to the data resulting in slope and intercept coefficients, e.g.,

$$Y = a + b*X \tag{1}$$

where Y is the new sensor (F-17 SSMIS) and X is the old sensor (F-13 SSM/I). Regressions were done for each daily. While there was some day-to-day variation in the regression coefficients, the daily values were averaged to produce average coefficient values (Table 3).

The regression coefficients were then used to adjust the F-13 tiepoints for the F-17 brightness temperatures (Tables 4 and 5). *Cavalieri et al.* (1999) found that this procedure did not yield sufficiently consistent sea ice fields, so they did a subjective manual adjustment of some of the tiepoints, particularly the open water (OW) tiepoints. In Cavalieri et al., this ‘tuning’ was done subjectively. There is inherent subjectivity in the procedure because (1) there is not necessarily a unique combination of adjustments that minimize the differences, and (2) it is not possible to minimize errors in both the total extent and total area estimates simultaneously.

Channel	Slope (*b*)	Intercept (*a*)	Std. Error
	Northern Hemisphere		
19V	0.982	5.098	1.80
19H	0.990	2.494	2.95
37V	0.980	5.655	3.50
	Southern Hemisphere		
19V	0.985	4.118	2.02
19H	0.992	1.686	3.38
37V	0.980	5.739	4.23

Table 3. Mean regression coefficients for brightness temperatures comparison between F-13 SSM/I and F-17 SSMIS. Std. Error = RMS($Y-Y_{est}$).

Here we used a more methodical procedure to reduce the subjectivity in the adjustment process. A cost function was defined (Equation 2), which was then minimized via a bracketed iterative approach.

$$\text{Cost} = A*f(\text{Extent}_{\text{summer}}) + B*f(\text{Extent}_{\text{winter}}) + C*f(\text{Area}_{\text{summer}}) + D*f(\text{Area}_{\text{winter}}) \qquad (2)$$

where f(X) is a function evaluating the difference in the given parameter. Here RMS and Mean Difference functions were used. For each iteration, a full year of daily total sea ice extent and area were calculated for F-17 and compared to the original F-13 values varying four of the tiepoints: the three open water tiepoints and the 37V FYI/A tiepoint. The initial iteration was centered on zero (no change between F-17 and F-13). For each subsequent iteration, the new interval was centered on the coefficient values that minimized the cost function from the previous iteration. At each iteration, the interval was halved, so that through the iteration process honed in on the optimal set of coefficients. The iterations continued until the interval reached 0.1 K, which is the radiometric resolution of the sensors.

Northern Hemisphere	F13	F17 Regression	Adjustment	Final F17
19V OW	185.2	186.9	-4.7	182.2
19H OW	114.4	115.7	+0.8	116.5
37V OW	205.2	206.7	-0.2	206.5
19V FYI	251.2	251.7		251.7
19H FYI	235.4	235.4		235.4
37V FYI	241.1	241.9	+0.8	242.7
19V MYI	222.4	223.4		223.4
19H MYI	198.6	199.0		199.0
37V MYI	186.2	188.1		188.1

Table 4. Northern Hemisphere tiepoints for F13 and F17 in Kelvin. Columns from left to right: (1) Tiepoint parameter; (2) F13 tiepoints; (3) F17 tiepoints derived from a regression analysis; (4) Adjustments made to the regression tiepoints to minimize extent and area differences between F17 and 13; (5) Final F17 tiepoints after the adjustment is made to the tiepoints from the regression analysis.

Southern Hemisphere	F13	F17 Regression	Adjustment	Final F17
19V OW	186.0	187.2	+0.5	187.7
19H OW	117.0	117.7	+0.7	118.4
37V OW	206.9	208.5	+0.4	208.9
19V A	256.0	256.2		256.2
19H A	241.4	241.1		241.1
37V A	245.6	246.4	+0.0	246.4
19V B	246.6	246.9		246.9
19H B	214.9	214.8		214.8
37V B	211.1	212.6		212.6

Table 5. Southern Hemisphere tiepoints for F13 and F17 in Kelvin. Columns from left to right: (1) Tiepoint parameter; (2) F13 tiepoints; (3) F17 tiepoints derived from a regression analysis; (4) Adjustments made to the regression tiepoints to minimize extent and area differences between F17 and 13; (5) Final F17 tiepoints after the adjustment is made to the tiepoints from the regression analysis.

The mean and RMS difference using several combinations of coefficients (A-D) were tested. It was found that using the RMS difference with equal weighting between coefficients (i.e., A = B = C = D = 0.25) provided the best overall results. Using an RMS difference accounts for the spread of the difference instead of simply the overall bias and RMS gives more weight to larger differences. There was little difference in the results using different weighting coefficients.

The calculated adjustments and the final F-17 tiepoints are provided in Tables 4 and 5. The daily differences in total extent and area are shown in Figures 1 and 2. The regression and adjustment has a small, but not negligible effect on the total extent estimates, but the largest effects are on the total area estimates, which are substantially improved by the regression and adjustments.

Northern Hemisphere	Total		Summer (6/1-8/31)		Non-Summer	
	10^6 km^2	*%*	*10^6 km^2*	*%*	*10^6 km^2*	*%*
Extent						
Mean	0.0044	0.052	0.0090	0.100	-0.0094	-0.136
RMS	0.0172	0.195	0.0155	0.167	0.0214	0.301
Max. Abs.	0.0588	1.053				
Area						
Mean	-0.0020	-0.029	-0.0033	-0.043	0.0020	0.041
RMS	0.0190	0.256	0.0187	0.232	0.0201	0.399
Max. Abs.	0.0796	1.054				

Table 6. Northern Hemisphere F17-F13 total sea ice extent and area difference.

With the adjusted tiepoints, the extent and area differences between F-13 SSM/I and F-17 SSMIS are small (Tables 6 and 7). The mean differences are on the order of 10,000 km^2 and RMS differences are on the order of 40,000 km^2. This puts the differences with the range the sensitivity of the brightness temperature measurements and the NASA

Team algorithm. Thus the consistency between the F-13 and F-17 timeseries is within limits of the sensor and algorithm capabilities.

The maximum absolute differences are all under 100,000 km2, which is reasonable. Concentration difference fields for the dates of maximum absolute differences (largest overestimation and underestimation by F-17 relative to F-13) shows that differences were generally small except near the ice edge (Figure 3). The larger differences appear in the Northern Hemisphere near spring and fall, where diurnal effects are largest. There also appear to be possible effects in regions toward the south where the limited number of overpasses per day can lead to greater diurnal effects (e.g., in Hudson Bay on 19 May). In the Southern Hemisphere, the differences are largest near the solstices. This may be a reflection of the impact on fast-changing ice conditions having a larger influence in the Antarctic than diurnal effects.

Southern Hemisphere	**Total**		**Summer (12/1-3/31)**		**Non-Summer**	
	10^6 km^2	*%*	*10^6 km^2*	*%*	*10^6 km^2*	*%*
Extent						
Mean	-0.0150	-0.131	-0.0236	-0.166	0.0025	0.043
RMS	0.0316	0.252	0.0329	0.225	0.0290	0.430
Max. Abs.	0.0844	1.639				
Area						
Mean	-0.0054	-0.063	-0.0091	-0.082	0.0020	0.055
RMS	0.0322	0.333	0.0347	0.304	0.0264	0.617
Max. Abs.	0.0736	1.605				

Table 7. Southern Hemisphere F17-F13 total sea ice extent and area difference.

Seasonality of Intersensor Calibration and Implications for Previous Sensor Overlaps

It is quite clear in Figures 1 and 2 that there is a seasonal signal in the intercalibration due to diurnal effects on the different sensors. This is likely due to differences in overpass times between the satellites and the effect of melt and other surface effects. In the Arctic the largest differences are generally found in the summer melt period. In the Antarctic, there is bimodal pattern, with the largest differences in the late-winter/early-spring and the late-fall/early-winter.

By having the full year for intercomparison, it is apparent that improvements could be made by using seasonal tiepoints and conducting intercalibration by season. This was done here to be consistent with the previous SMMR-SSM/I approach.

However, the seasonal effect has likely had an effect on the efficacy of the previous intercalibrations because the overlap periods were very short and thus only encompassed part of the full seasonal cycle. Having the full year does afford us the opportunity to investigate these effects. We did this by using only a subset of the full year F17-F13 overlap corresponding to the previous sensor overlap periods and redoing the F17-F13 intercalibration. The intercalibration methodology to derive new tiepoints was the same, except over the limited time period. Then the new “short-interval” tiepoints were used to

produce the full year of sea ice extent and areas. The differences were then compared with the full year interval.

This comparison does not necessarily provide a direct error estimate of the previous sensor intercalibration because the sensor characteristics are different as are the physical environmental conditions (e.g., concentration, onset of melt, other surface emissive properties). However, it does suggest the sensitivity of the intercalibration to the time interval of the overlap and the potential limitations of having only a short overlap period.

Total area was most affected by the change in time periods with the shorter overlap periods yielding larger differences (less consistency) compared to using the full year overlap period (Table 8). Extent showed similar behavior, but with smaller magnitude differences. This is not unexpected and others (e.g., *Cavalieri et al.*, 1999) have commented on needing at least a full year of overlap for an optimal intersensor calibration.

	Northern Hemisphere		**Southern Hemisphere**	
	Mean	*RMS*	*Mean*	*RMS*
Full Year (4/1 – 3/31)	-0.0020	0.0190	-0.0054	0.0322
F13-F11 Overlap (5/30 – 9/30)	-0.0185	0.0307	-0.0043	0.0347
F11-F8 Overlap (12/3 – 12/18)	0.0223	0.0309	-0.0604	0.0711
F8-SMMR Overlap (7/9 – 8/20)†	-0.0120	0.0295	-0.0204	0.0384

Table 8. Mean and RMS average total area difference in km2 using different overlap periods to derive new F-17 tiepoints. †SMMR collected data every other day.

Larger magnitude differences did not necessarily correspond with shorter overlap periods. It appears the season of the overlap period plays a role. In the Antarctic, the overlaps periods during the austral winter (F13-F11 and F8-SMMR) yielded better results than the summer. In the Arctic, this difference isn't apparent in the summary statistics (Table 8), possibly because there isn't a true boreal winter period. However, the closest period, during December for F11-F8, does show lower magnitude differences through much of the year except during the peak summer melt season (Figure 4) where, as expected, the summer overlap is much more successful and reducing the differences.

It is hoped that future intercalibrations can be conducted for a full year as this clearly provides superior results. However, the results here show that if a full year is not available, the timing of the overlap can be important in the overall quality of the intercalibration.

Conclusion

An intersensor calibration of sea ice fields from F-17 SSMIS with F-13 SSM/I has been completed for NSIDC near-real-time sea ice products. The calibration yields good

consistency between the two products, providing confidence in a consistent long-term data record.

Sensitivity tests were done to determine the potential effects from using shorter intervals for intersensor calibration as were employed for previous SSM/I and SMMR transitions. The shorter intervals resulted in less consistency confirming previous assessments that using a full year overlap is essential to provide optimal consistency. There is also a clear seasonal signal in the full year overlap, suggesting that using seasonal tiepoints and conducting intercalibration for each individual season could result in a more consistent timeseries.

References

Cavalieri, D.J., P. Gloersen, and W.J. Campbell, 1984. Determination of sea ice parameters with the Nimbus 7 SMMR, *J. Geophys. Res.*, vol. 89, pp. 5355-5369.

Cavalieri, D., C. Parkinson, P. Gloersen, J. Comiso, and H. Zwally,1999. Deriving long-term time series of sea ice cover from satellite passive-microwave multisensor data sets, *J. Geophys. Res.*, 104(C7), 15803-15814.

Comiso, J.C., D.J. Cavalieri, C.L. Parkinson, and P. Gloersen, 1997. Passive microwave algorithms for sea ice concentration: a comparison of two techniques," *Rem. Sens. Environment*, vol. 60, pp. 357-384.

Wentz, F., 1997. A well-calibrated ocean algorithm for special sensor microwave/imager, *J. Geophys. Res.*, 102(C4), 8703-8718.

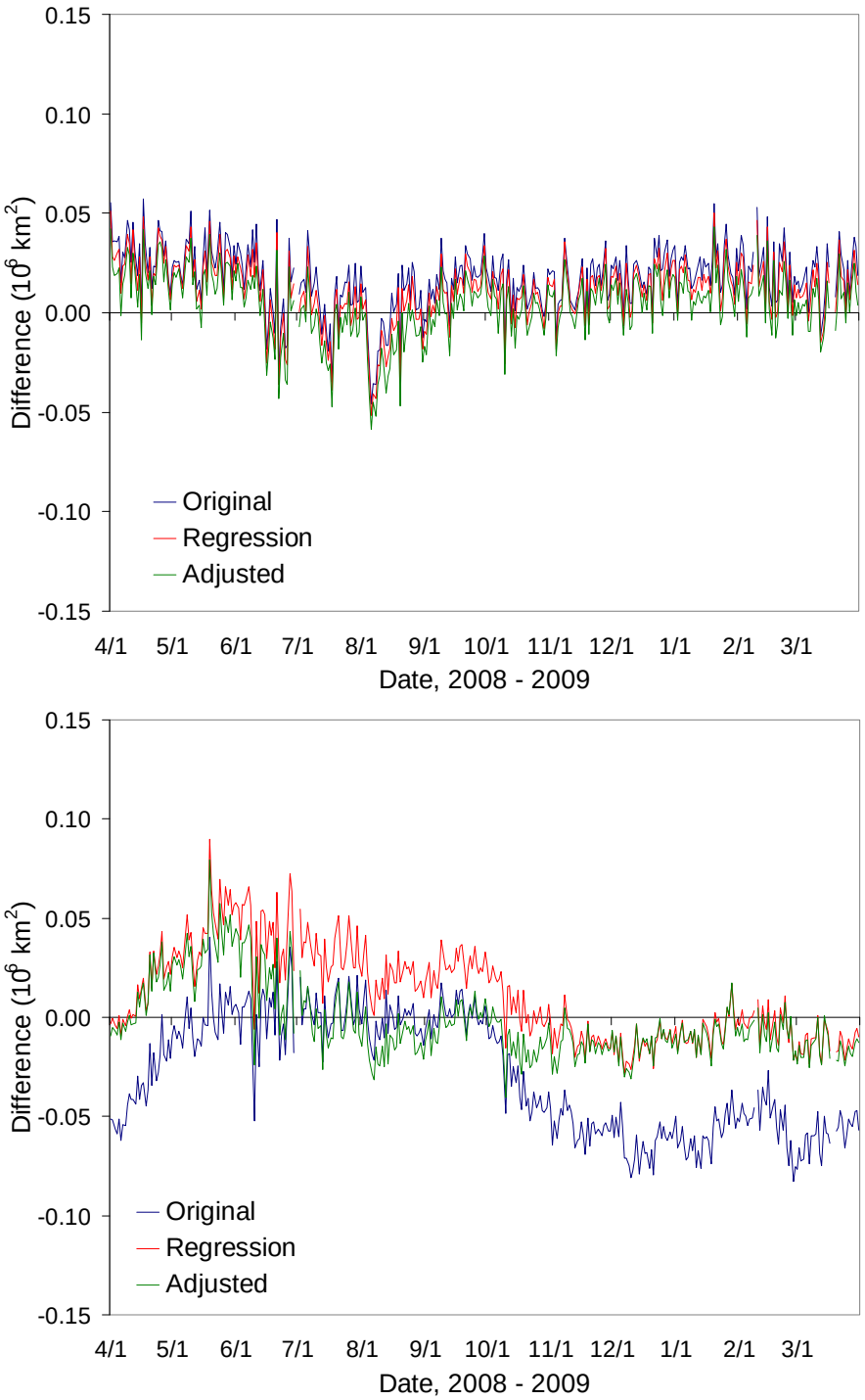

Figure 1. Northern Hemisphere daily total sea ice extent (top) and sea ice area (bottom) difference between F-17 SSMIS and F-13 SSM/I using: (blue) original F-13 tiepoints, (red) tiepoints from regression, and (green) adjusted tiepoints.

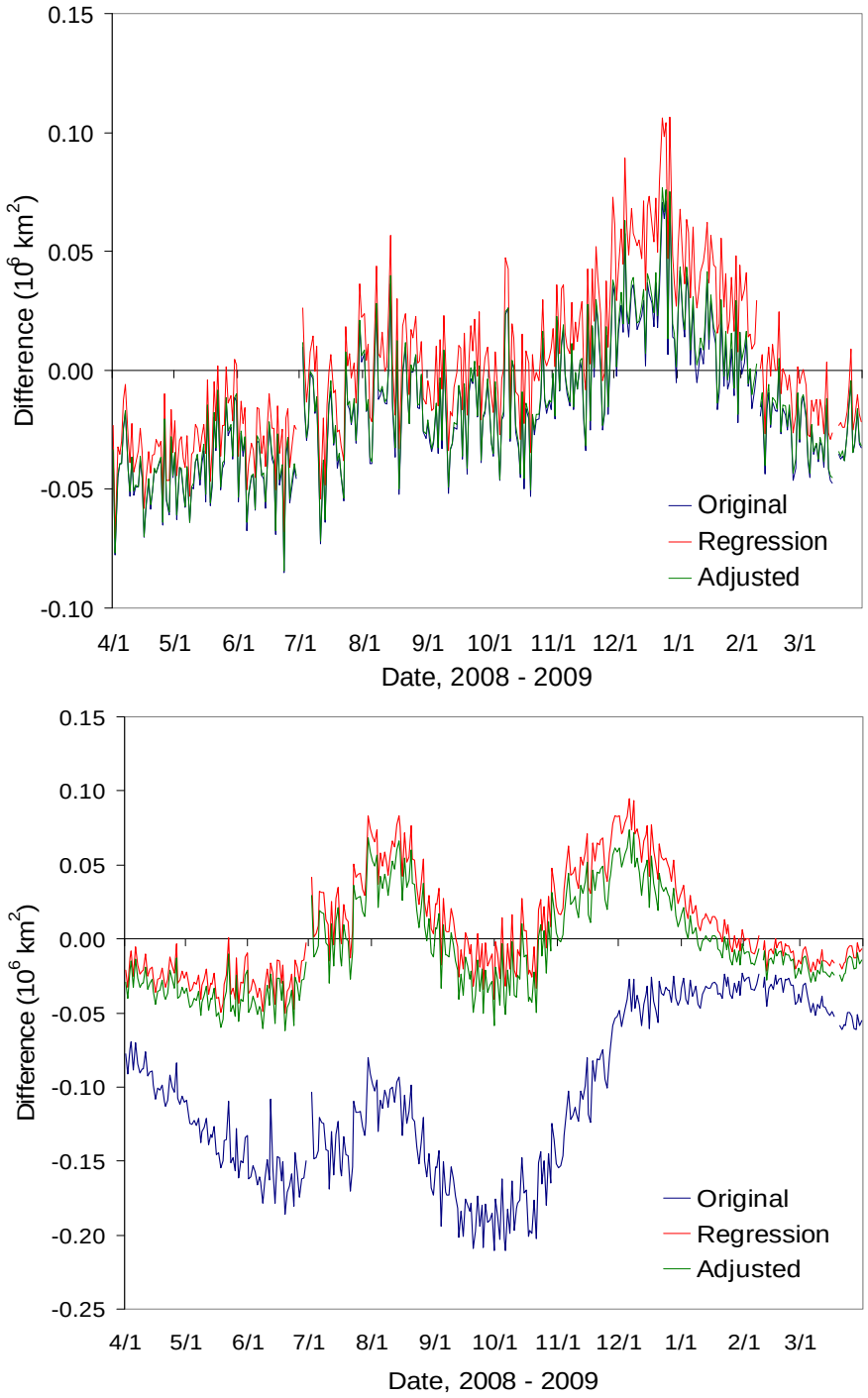

Figure 2. Southern Hemisphere daily total sea ice extent (top) and sea ice area (bottom) difference between F-17 SSMIS and F-13 SSM/I using: (blue) original F-13 tiepoints, (red) tiepoints from regression, and (green) adjusted tiepoints.

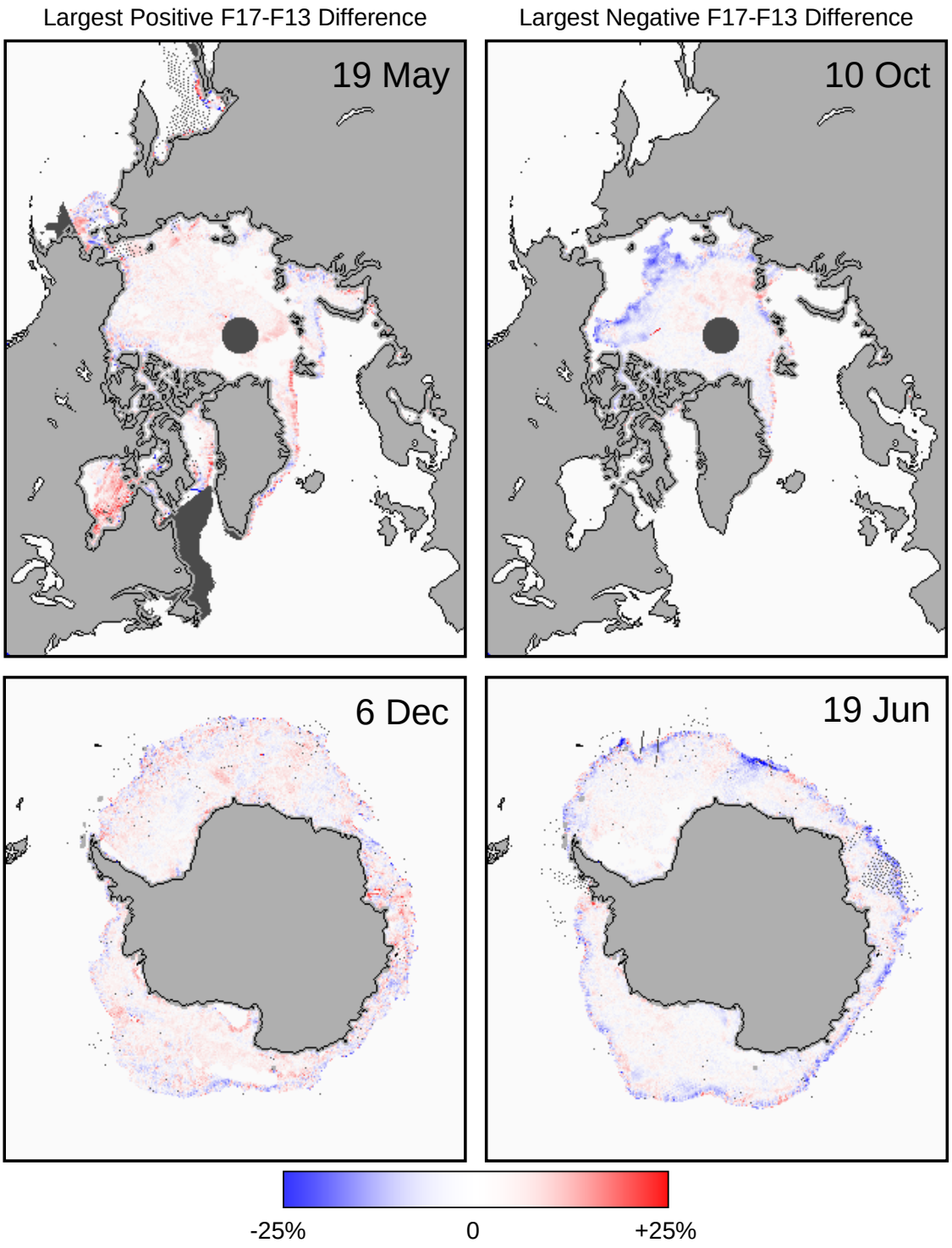

Figure 3. Sea ice concentration difference, F17-F13 dates of (left) largest positive difference (i.e., F17 > F13) and (right) largest negative difference (i.e., F13 > F17). All dates are in 2008.

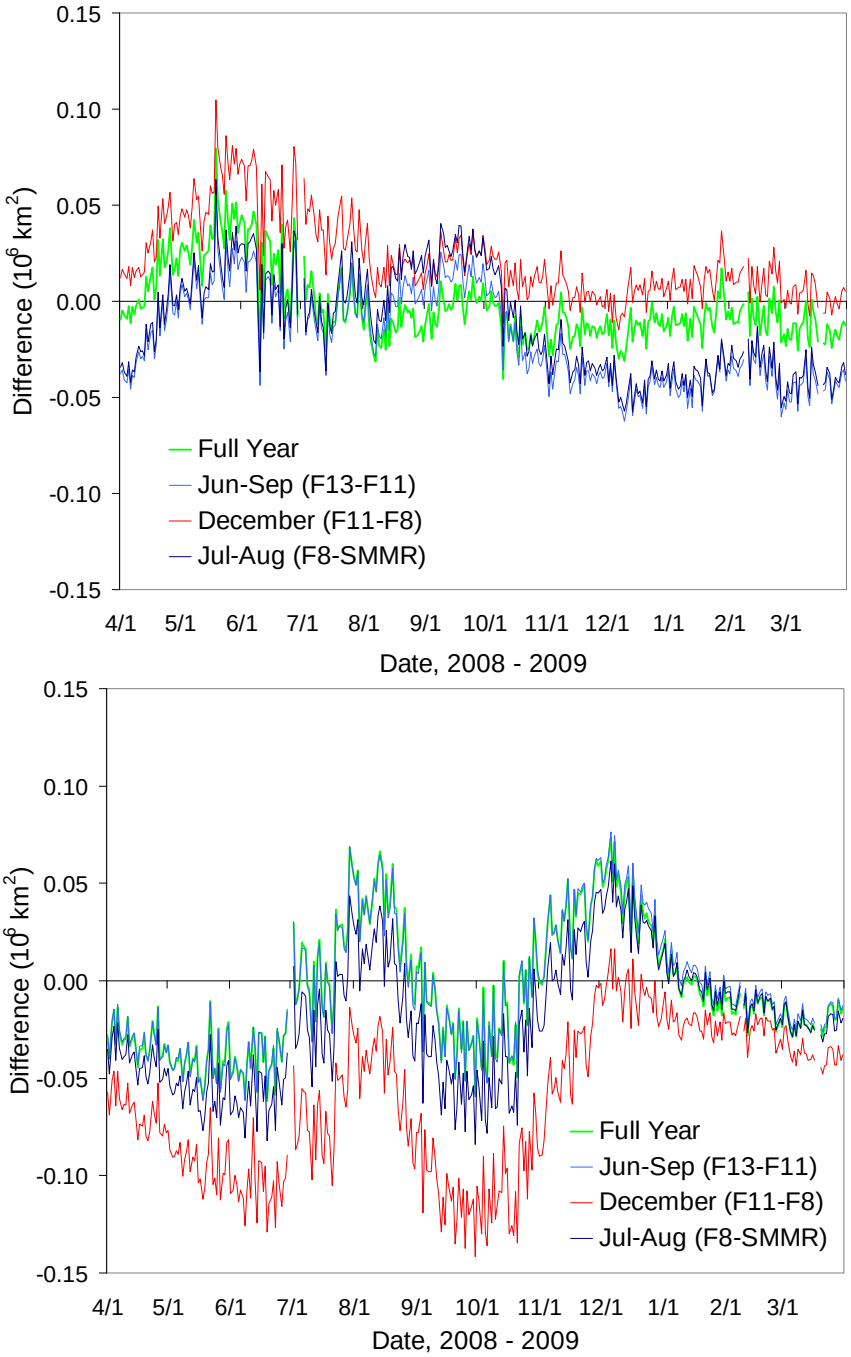

Figure 4. Northern hemisphere (top) and Southern Hemisphere (bottom) daily total sea ice area difference between F-17 SSMIS with adjusted tiepoints and F-13 SSM/I using an overlap period of: (green) full year, (light blue) Jun-Sep F-13-F11, (red) December F11-F8, and (dark blue) July-August F8-SMMR.